AEROACOUSTICS INVESTIGATIONS OF A WIND TURBINE FOR DIFFERENT VELOCITIES USING COMPUTATIONAL FLUID DYNAMICS SOFTWARE

Haydar KEPEKCI
Department of Mechanical Engineering, Beykent University, Istanbul, Turkey
haydarkepekci@beykent.edu.tr

Baha ZAFER
Department of Mechanical Engineering, Istanbul University, Istanbul, Turkey
baha.zafer@istanbul.edu.tr

Hasan Rıza GUVEN
Department of Mechanical Engineering, Istanbul University, Istanbul, Turkey
hrguven@istanbul.edu.tr

Abstract

The main reason why wind farms cannot be installed close to people's habitats is the noise pollution they generate while working. This paper studies a flow area, which is analyzed on the 3D S809 blade profile using the SST k-ω turbulence model to calculate the near-field flow of wind turbines. The attached a time-dependent flow field factors in Ffowcs-Williams and Hawkings (FW-H) equating Sound Pressure Level (SPL) was calculated for different velocities as 5.4 m/s and 7 m/s from the microphone placed in the computational domain to be analyzed. In this study, the NREL phase VI small scale (12%) baseline airfoil type was used. The acoustic results and torque values obtained from the analyzes were compared both with the data in the literature and among themselves. As a result; one of the calculated torque values was under the literature amount. This differentiation maybe since the analysis given in the literature contains a higher number of mesh

cells. SolidWorks software was used for airfoil drawing, and Ansys Fluent software was preferred for analysis in research. This article involves a subject that is on the near-field flow of wind turbines. This sample of 3D S809 has nearly 2.2 million elements and solves compressible fluid flow with the SST model. The same mesh geometry was used in both analyses.

Keywords

Acoustics, FW-H Equations, SST, S809, NREL Phase VI, Wind Turbine, Renewable Energy

1. Introduction

Changing climate is progressively recognized kind of one of the several difficulties all the time to confront humanity. To decrease greenhouse gas radiations which conduce to climate alteration, a requisition in order to renewable energy is rising because of international arrangement lately. The impact of climate change, which is evident from observations of rising temperature, melting snow, and rising sea levels, has stressed the importance of low carbon-emission energy sources (Worasınchai, 2012). The worry about global warming has instigated a renovated interest in renewable energy sources. Wind energy is one of the sources that play a significant part in electricity generation, and the use of wind turbines to provide electricity has proliferated recently (Global Wind Energy Council, 2010).

Though wind turbines might seem like an excellent resolution to produce renewable energy, the discussion happens regarding the installation of wind turbines close to resided areas, owing to rumble annoyance. Managements implement rumble ordinances for supreme permissible sound levels for wind turbines near populated areas. Those noise regulations cut off the capacity throughput of wind turbines that leads to a decrease in yearly energy generation (Rooks, 2016). In order to overcome this problem, the issue of optimizing the noise generated from wind turbines has been come up. Recently varied types of research have been managing to measure the wind turbine sound. The source of wind turbine sound might be separated into different major categories, i.e mechanical, and aeroacoustic noise. Various parts produce mechanical noise in the middle, like noise from the gearcase. The aeroacoustic noise of a wind turbine is produced by the interplay within the coming wind and the tower and the rotor blades. The spread of mechanical noise might be decreased by doing sufficient insulation.

Nevertheless, the spread of aeroacoustic sound resources is not simplistic. Since the noise resources are placed at the external of the blades making insulation and absorbent matters ineffective, to decrease the aeroacoustic sound, the resources ought to be reduced that includes

complicated devices. For In order to wind turbines, aeroacoustic rumble is the very predominant sound resource, also ahead of comprehension of the devices is essential to decrease noise radiations (Oerlemans, 2007).

Aeroacoustic resources classified as monopole, dipole, and quadrupole. Monopole and dipole sources; are welded close to the surfaces and are strong emitters of acoustic energy. Quadrupole sources are welded far from the surfaces and are low emitters. For instance; an exceptionally turbulent flow can be produced by the wind turbine. Aerodynamic noise created by the wind turbine; is owing to the unbalanced inflow at the plane of the blade that reasons powerful resources (Kepekci et al., 2018). Various aeroacoustic sources can be associated with the noise generation of wind turbines, most of them are owing to the interplay within the coming wind with the wind turbine blades that acknowledged like airfoil self-noise. The blade self-noise is occasioned via the interplay within the airfoil facade and its own borderline zone. According to (Brooks et al., 1989) various kinds of airfoil self-noise procedures and sound generation in wind turbines existing that are shown in Fig. 1.
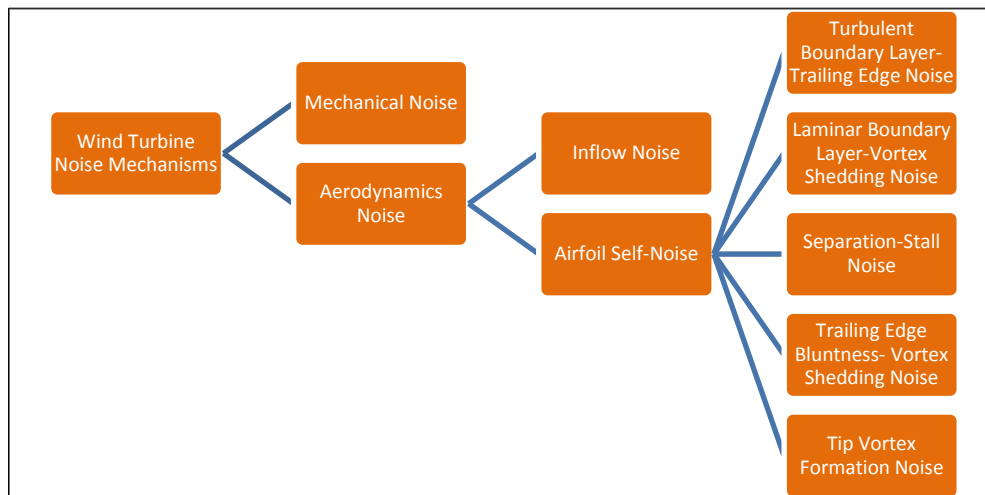

Figure 1: *Sound Generation in Wind Turbines*

As an alternative to empirical methods, Computational Flow Dynamics and Computational Aeroacoustic Methods are used. In order to the accurate forecast of sound generation in a wind turbine; close to the surface of the blade needs useful solution transient flow field data. Process suchlike either Large Eddy Simulation (LES) or Direct Numerical Simulation (DNS) may be applied to compute the unsteady turbulent flow area. The primary necessity of such solution methods is fine mesh particles around the airfoil surface (Wasala et al., 2015). DNS (Direct Numerical Simulation) approach is the best way to gather any base turbulence configuration that

are essential in the acoustic subject. DNS has the skill to solve any little turbulence configuration outside any modeling. Nevertheless, DNS is much expensive in conditions of calculation period; it requires a highly pure meshes solution to solve the whole turbulent height measure (Tadamasa & Zangeneh, 2011).

1.1 Literature Research

Morris et al. (2004); put forwarded computational methods for the predicted of aeroacoustic sounds. The principle of the methods; it is derived from on low-frequency noise from the tail edge noise. Handling unstable flow simulations, the Ffowcs Williams-Hawkings formularization combined noise field diffusion. They used linearized Euler equations for long-range noise diffusion prediction. Jianu et al. (2012); examined developments in the field of sound pollution from turbines. His work principally focused on investigating and comparing various approaches used to decrease sounds, focusing on the noise coming from the tail edge. They also talk about repression of sounds from mechanical causes such as generators, transmission and hydraulic systems using vibration suppression, vibration insulation, and error detection techniques. According to this study; prevention strategies such as blade forming designs in wind turbines can decrease the dominant noise.

Velden et al. (2016) analyzed both the flow field and the noise emission at the curved tail edge both experimentally and numerically. Computation was made using the Lattice Boltzmann equation with the Ffowcs William Hawking aeroacoustic analogy and noise forecast was acquired. To validate this methodology used for edge noise prediction, the low Mach number flow around the plain plate with a 25-degree incline tail edge was examined. The data acquired from the experimental analysis were compared, and the consequences received showed a well suitable.

Avallone et al. (2017) created a serrated tail edge and investigated the far-field noise and the flow zone. They got the spectrum of the far-field broadband sound and the flow area out of mathematical estimates using compressible Lattice-Boltzmann. They compared the renewed style with the classic saw-type tail edge with triangular geometry. They applied both geometries to the NACA 0018 wings at a 0-degree angle of attack. Consequently, they found that the serrated geometry decreased the noise of the broadband by about 2 dB compared to the classic design. This was because the serrated edge reduced the scattered noise at the root. Maizi et al. (2017) studied the impression of blade tip shape on sound radiation out of the flat axle wind turbine. In their numerical study, they used the S809 airfoil used in the NREL phase IV experiment. They used Detached Eddy Simulations method in three-dimensional flow simulation. As a result, they

obtained the best results using the shark tip. They thought that the reason for this result was the reduction of the turbulence effect in the airfoil tip region.

1.2 Purpose of the Study

In the study, S809 blade profile was created for the rotational domain of wind turbine. The required blade profile drawing was made using the SolidWorks program. SolidWorks is an innovative, easy-to-use three-dimensional design program. SolidWorks enables the user to draw quickly in any machine, plant, product design. The appropriate mesh is prepared with the Ansys Workbench program. ANSYS Fluent is a program that can perform fluid dynamics calculations. ANSYS Fluent, which is used for air and water analysis of vehicles such as aircraft, ships, and automobiles, provides the opportunity to create a comprehensive flow simulation by creating and calculating mesh acting like a fluid. It was simulated using ANSYS Fluent with the SST k-ω method.

For the acoustic value measurements, 18 microphones with a 1 m radius were situated at a space of 1.88 m from the middle of the wind turbine blades and a length of 1.49 m. Since the microphones are placed on a circle axis, there is an angle of 20 degrees between each. The values received from different microphones are compared with each other. So, the field that is most likely to be disturbed is seen. From the experiments carried out for NREL phase IV, the sound pressure level amounts at different wind inlet velocity were found for the basic blade form. The main aim of this study is the research of the impressions of the different velocity inlet on noise radiation from wind turbines utilizing the aeroacoustic type for decrease sound radiation created ex adverse impact on power amount. The aeroacoustic and close area sound nearby the wind turbine generating set is straight examined utilizing Unsteady Reynolds-averaged Navier Stokes (URANS) model. Ffowcs Williams-Hawkings (FW-H) analogy is used in the estimate of the far-field sound at specific situations far away from the wind turbine blades. A full confirmation has been put forward in this study with present test data for a little scale wind turbine of NREL Phase VI.

2. Numerical Method

2.1 Reynolds-Averaged Navier-Stokes Equations

The incompressible Navier-Stokes equations in conservation form are

$$\frac{\partial u_i}{\partial x_i} = 0 \qquad (1)$$

$$\rho \frac{\partial}{\partial x_j}\left(u_j u_i\right) = -\frac{\partial p}{\partial x_i} + \frac{\partial}{\partial x_j}\left(2\mu s_{ij}\right) \quad (2)$$

Where $s_{ij} = (1/2)\left(\partial u_i/\partial x_j + \partial u_j/\partial x_i\right)$ is the tensor of strain-rate. Accordingly, Eq. (2) reword as follows as

$$\rho u_j \frac{\partial u_i}{\partial x_j} = -\frac{\partial p}{\partial x_i} + \mu \frac{\partial^2 u_i}{\partial x_i \partial x_j} \quad (3)$$

Considering to turbulent flow characteristics, the field variables u_i and p must be expressed as the sum of the mean and fluctuating parts as

$$u_i = U_i + u'_i. \, p = P + p' \quad (4)$$

With the bar denoting the time average. By inserting these definitions into Eqs. (1) so (2), the Eqs. (4) also, (5) are obtained as follows:

$$\frac{\partial U_i}{\partial x_i} = 0 \quad (5)$$

$$\rho \frac{\partial}{\partial x_j}\left(U_j U_i\right) = -\frac{\partial P}{\partial x_i} + \frac{\partial}{\partial x_j}\left(2\mu S_{ij} - \overline{\rho u'_i u'_j}\right) \quad (6)$$

In that $S_{ij} = (1/2)\left(\partial U_i/\partial x_j + \partial U_j/\partial x_i\right)$ and $\tau_{ij} = \overline{-u'_i u'_j}$ are the mean strain-rate tensor and the Reynolds stress tensor, separately. Using these two quantities, the Eq. (6) is written as follows.

$$U_j \frac{\partial U_i}{\partial x_j} = -\frac{\partial P}{\partial x_i} + v \frac{\partial^2 U_i}{\partial x_i \partial x_j} - \frac{\overline{\partial u'_i u'_j}}{\partial x_j} \quad (7)$$

Also, there are various turbulence models in order to describe obscure quantities. In the present paper, k-ω SST is used to reach this aim.

2.2 Turbulence Model

The K- ω model is a two-equation turbulence model that occur in two additional transport equations like this turbulent kinetic energy (k) that determines the energy in the turbulence as fine as the particular spreading (u) that foretells the turbulence measure, to show the turbulent characteristic of a turbulence flow. Additionally, the shear stress transport (SST) k-u turbulence model is a two-equation eddy-viscosity model that has identified. (Menter, 1994). For the inner parts of the boundary layer, this model uses a k-u formulation. Accordingly, these properties of (SST) k-u turbulence model, this model is usable down to the wall through to the viscous sub-layer. For this reason, the SST k-u model can be applied for turbulence flows with low Reynolds number without that additional damping functions. Moreover, the SST formulation also can couple with the k-ε model in the free-stream that helps the model to decrease the sensitivity to the inlet free-stream turbulence characteristics. The other utility of the SST k-u model is well to foresee the reverse pressure gradients and separating flow. The SST k-u model does generate a bit too massive

turbulence levels in regions with large normal strain, like recession regions and regions with strong acceleration. In this method, the turbulence kinetic energy, and specific dissipation rate compute as follows:

$$\frac{\partial k}{\partial t} + U_j \frac{\partial k}{\partial x_j} = P_k - \beta^* k\omega + \frac{\partial}{\partial x_j}\left[(v + \sigma_k v_T)\frac{\partial k}{\partial x_j}\right] \quad (8)$$

$$\frac{\partial \omega}{\partial t} + U_j \frac{\partial \omega}{\partial x_j} = \alpha S^2 - \beta\omega^2 + \frac{\partial}{\partial x_j}\left[(v + \sigma_\omega v_T)\frac{\partial \omega}{\partial x_j}\right] + 2(1 - F_1)\sigma_{\omega2}\frac{1}{\omega}\frac{\partial k}{\partial x_j}\frac{\partial \omega}{\partial x_i} \quad (9)$$

where the kinematic eddy viscosity,

$$v_T = \frac{a_1 k}{\max(a_1\omega, SF_2)} \quad (10)$$

Moreover, the closure coefficients and auxiliary relations are described as follows;

$$F_2 = tanh\left\{\left[max\left(\frac{2\sqrt{k}}{\beta^*\omega y}, \frac{500v}{y^2\omega}\right)\right]^2\right\} \quad (11)$$

$$F_1 = tanh\left\{\left[min\left(max\left(\frac{2\sqrt{k}}{\beta^*\omega y}, \frac{500v}{y^2\omega}\right), \frac{4\sigma_{\omega2}k}{CD_{k\omega}y^2}\right)\right]^4\right\} \quad (12)$$

$$P_k = min\left(\tau_{ij}\frac{\partial U_i}{\partial x_j}, 10\beta^* k\omega\right) \quad (13)$$

$$CD_{k\omega} = max\left(2\rho\sigma_{\omega2}\frac{1}{\omega}\frac{\partial k}{\partial x_i}\frac{\partial \omega}{\partial x_i}, 10^{-10}\right) \quad (14)$$

$$\emptyset = \emptyset_1 F_1 + \emptyset_2(1 - F_1) \quad (15)$$

Also, the constant values are as follows:

$$\alpha_1 = \frac{5}{9}, \alpha_2 = 0.44, \beta_1 = \frac{3}{40}, \beta_2 = 0.0828, \beta^* = 0.09, \sigma_{k1} = 0.85, \sigma_{k2} = 1, \sigma_{\omega1} = 0.5, \sigma_{\omega2}$$
$$= 0.856$$

2.3 Acoustic Analogy Methods

The aeroacoustic estimate pattern is based on the Ffowcs Williams Hawkings (FW–H) equation (Ffowcs Williams & Hawkings, 1969) that is the greatest common formulation of the Lighthill acoustic analogy (Lighthill, 1952). This interests the difficulty of noise produced by a body in free movement in both period and periodicity fields. FW-H equation has been generally utilized for the accomplished estimate of rotor and blades. The FW-H equation is based on an analytic description that links the far-field pressure to integrals above an enclosed facade that round totals the acoustic resources. The equality (FW–H) is a rearrangement of the persistence equation. The Navier-Stokes (N-S) equations into an inhomogeneous stream equalization with resources of noise like shown in the form of Eq. (16)

$$\frac{1}{{a_0}^2}\frac{\partial^2 p'}{\partial t^2} - \nabla^2 p' = \frac{\partial}{\partial t}\left[(\rho_0 V_n + \rho(U_n - V_n))\delta(f)\right] - \frac{\partial}{\partial x_i}\left[\left(P_{ij}n_j + \rho u_i(U_n - V_n)\right)\delta(f)\right] +$$

$$\frac{\partial^2}{\partial x_i\,\partial x_j}\left[T_{ij}H(f)\right] \qquad (16)$$

Eq. (16) is a best-validated approach, which is utilized widely in rotorcraft aeroacoustics (Schultz, 1994). The first phrase on the right hand is a monopole source made by the unsteady mass injection, the second phrase is a dipole source by unsteady external forces, and the third term is a quadruple source caused by unsteady shear stresses. p' is the sound pressure in the far field. (f = 0) means a mathematical facade introduced to "surround" the external flow problem (f > 0) in an unlimited space that facilitates the utilization of generalized theory and the free-space Green equation to get the solution (Maizi et al., 2017).

The surface (f = 0) corresponds to the source (emission) surface (blade and shaft), n_j is the unit normal vector pointing toward the external area (f > 0). a_0 is the far-field sound speed, and T_{ij} is the Lighthill stress tensor as described :

$$T_{ij} = \rho u_i u_j + P_{ij} - {a_0}^2(\rho - \rho_0)\delta_{ij} \qquad (17)$$

u_i is fluid velocity element in the i direction and unit fluid velocity element normal to the surface f=0. V_{ij} is the surface velocity element in the x_i direction, and V_n is the surface velocity element normal to the surface. $\delta(f)$ is the Dirac delta function, $H(f)$ is a Heaviside function, P_{ij} is the compressive stress tensor (Jang&Young, 2011).

3. Blade Confirmation

The aeroacoustic pretending methodology was examined on an S809 blade type which created using SolidWorks. After the computations are finished, the results of NREL Phase VI experimental are compared data (Cho et al., 2009). The S809 blade type is aerofoil that is used NREL Phase VI by the National Advisory Committee for Aeronautics. It has been extensively utilized in the aerospace application for acoustic calculations in wind turbines. ANSYS Fluent has been applied to compute the aeroacoustic inflow parameters that needed being data to the FW-H equation. The confirmation of the flow solver has been enforced of the NREL Phase VI wind turbine model. An original model of phase VI experimental is at two blades zero cone angle. The geometry of the blade was elaborated in with a diameter of 10 m. Cho et al. tested a 12% scale of the original experiment at Aerospace Recherché institute in 2010. For numerical verification, the data we have obtained from our calculations were compared with their results.
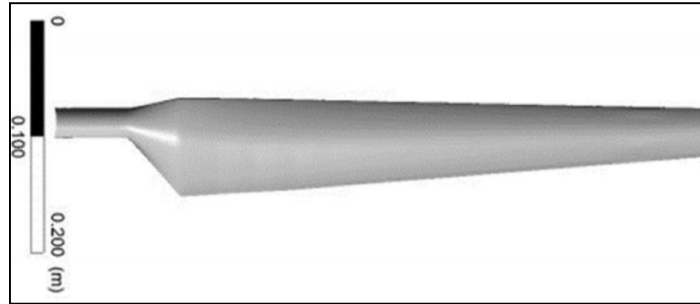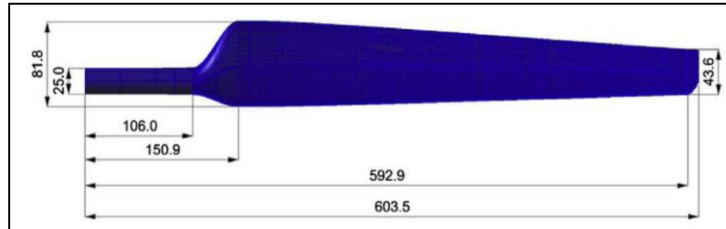
Figure 2: *Blade of the NREL Phase VI*

Figure 3: *Measurements of 12% Dimension of wind Turbine Blade used in the NREL Phase VI Experiment*

In this study, the steeple of the wind turbine and the floor impact are disregarded. That is an appropriate approach for HAWT rotor pretence. The computational domain is formed of one full and one half-cylindrical subdomain; one external fixed area with poor mesh. The computational field for the NREL phase VI area is surrounded within a less internal roll and an external semi-roll including a span equivalent to 3 times the rotor caliber. Therefore, the area is expanded to 8 rotor calipers down the wind of the turbine. The Ansys Workbench is utilized to produce the bulk mesh. This mesh structure contains about 2.2 million cells.
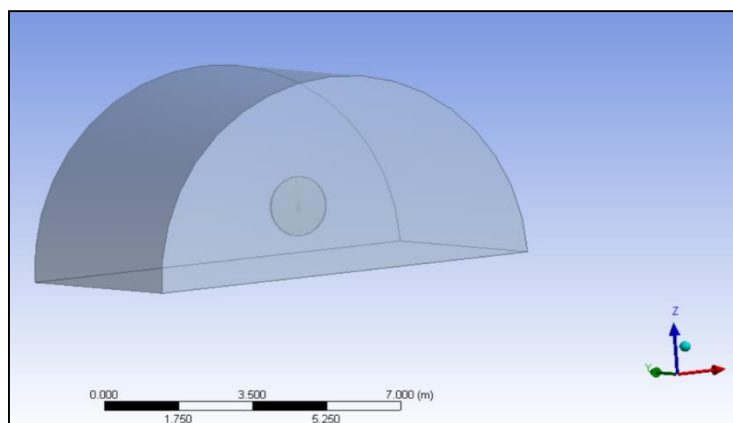

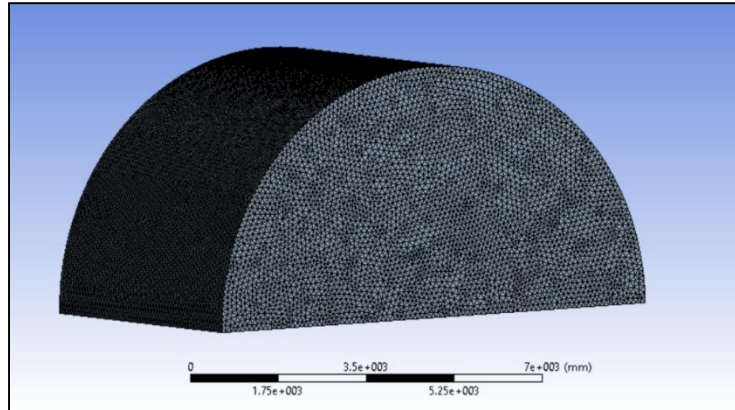**Figure 4:** *Computational Domain*

Figure 5: *Mesh Image of the Computational Domain created using Workbench*

Numerical analysis was performed to determine sound pressure levels and torque forces on the rotate wind turbine using Ansys Fluent program, two of which gave acceptable results. The difference of the analyzes; in one of them, the velocity of wind inlet velocity was taken as 7 m/s and in the other as 5.4 m/s. In both analyses, the nominal rotation speed was 600 rpm. When it is necessary to make a time-sensitive resolution for rotor-stator interplay, it is necessary to use a floating mesh model to calculate the unstable flow area. This model is the best exact way to simulate flows in many going reference support however is very difficult to calculate. Unstable solutions are periodic, which repeats itself after a while. It is known that it is more efficient to use a rotating reference frame when there is no cooperation within fixed and going pieces.

In our solution, we used a floating mesh structure. In a floating network technics, a lot of cell regions are utilized. All cubicle region is limited to at smallest one "interface region" to which it faces the opposite cubicle region. The interface regions of nearby cubicle regions interact with each other. These regions act together. During calculation, the cell regions rotate relative to each other. No node alignment is required during rotation. Because the flow is unstable, a time-dependent resolution method is needed (Ansys Fluent 12.0, Tutorial Guide). The working fluid for the study is the air with a density similar to the reference amount in the experiment info that is 1.2 kg/m^3. Concerning the borderline terms, a speed stipulation with a turbulent volume of 1% is utilized at the upriver limit. In the analysis, time-dependent Reynolds Navier-Stokes (uRANS) equalizations were done as a turbulence pattern. For uRANS solutions; SST k-ω method was used. The convergence criterion is 10-6 for all residuals. In the study, the time step was determined as 10^{-5}. Both analyzes were continued for 0.01 s.
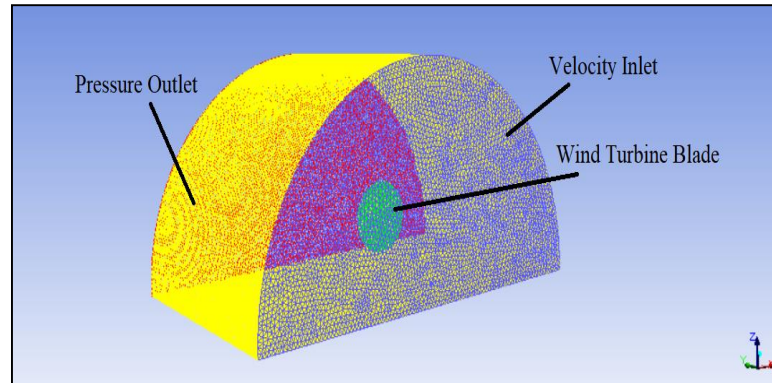
Figure 6: *Boundary Conditions*

4. CFD Results

On account to validate the analyses, a torque of horizontal force to the blade's surface was compared with experimental data. Firstly, the formulas used in the calculations, and then the graphs obtained from these comparisons are given below.

The following equation calculates the kinetic energy of air:

$$P_w = \frac{1}{2}\dot{m}V^2 \quad (18)$$

That $\dot{m}(kg/s)$ is the air mass flow rate, and $V(m/s)$ is the speed of blowing air. By replacing $\dot{m}$ energy equation is changeable to power in the surface that is swept by rotor:

$$P_w = \frac{1}{2}\rho v^3 A \quad (19)$$

P_w (watt) is power, ρ (kg/m^3) is air density and $A(\pi r^2)$ is a surface that is swept by rotor. Next Next equation is helpful to compute force generated by the turbine:

$$P_t(\theta) = F(\theta).v(\theta) = T(\theta).\omega(\theta) \quad (20)$$

θ is angular is an angular position of the turbine, T is the torque of vertical force to blade's surface, v is velocity vector in force point of F, and ω is rotating speed of the blade (Sargolzaei, 2007).
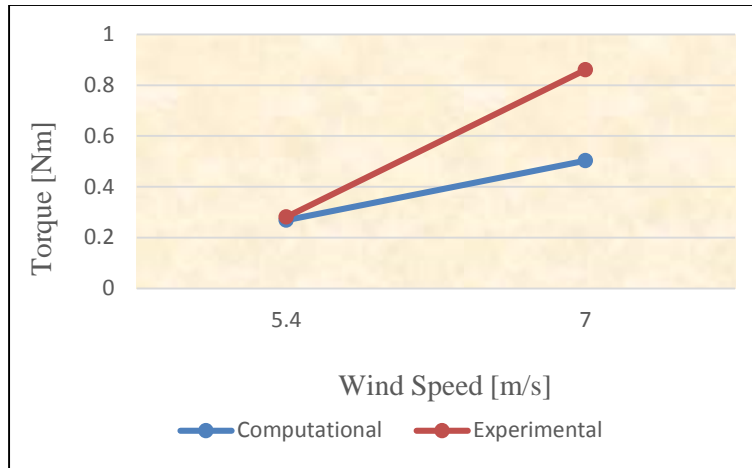
Figure 7: *Torque values SST- kω method results of 3D S809 blade compared with experimental data (Cho et al., 2009)*

For 3D S809 wind turbine blade type, two different wind speed values as 5.4 (m/s) and 7 (m/s) were used in this study. The torque results have been appraised for SST k-ω calculations at two different velocity values and it's shown in Fig. 7. When the experimental data (Cho et al., 2009) are compared, similar results were obtained for the calculation made for 5.4 (m/s); but numerical differences have been found in calculations made for 7 (m/s). The reason for this difference is thought to be the use of URANS method. For more precise calculation, LES or DES turbulence methods should be used.

4.1 Aeroacoustics Analysis

In the part, the aeroacoustic study is debated to appraise the sound emitted of the 12% scale model with various velocities. The inflow nearby the blades is computed utilizing the unstable flow area on the blade face removing from URANS model. The SST model is practiced in the current study to research the condition at turning speed 600 rpm (12% scale model) with various velocities 5.4 (m/s) and 7 (m/s). The period pace was limited at 10-5 seconds, and the pretense was done for a period time of 0.01 seconds, with almost two rotation blade for acquiring a correct estimate. While such a short time is not accepted to get a certain noise spectrum, it can be evaluated in terms of providing clues about the results. The sound pressure level (SPL) of the URANS calculations are calculated according to the following expression:

$$SPL_s = 20log\left(\frac{p'}{p_{ref}}\right) dB \qquad (21)$$

A total of 18 receivers were used in the analysis for S809 wind turbine blade. All microphones were placed evenly around the circle. Position of microphones placed on coordinate

axes; determined using the SolidWorks program. As shown in Figure 7, there is an angle of 20 degrees between each.
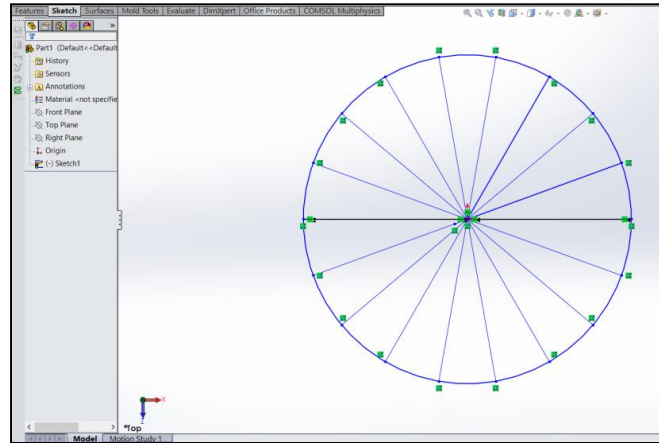

Figure 8: *Determining the Coordinates of Microphones placed around Wind Turbines*

For the URANS model, there is a huge important diversity in the pressure level noise within dipole and quadrupole source for the all range of frequencies. It is noted that the best energy noise radiation is of dipole nature (Maizi et al., 2017). The comparison of the Sound Pressure Level obtained from the analysis with a wind speed of 7 m/s with experimental data (Cho et al., 2009) is shown in Figure 9.
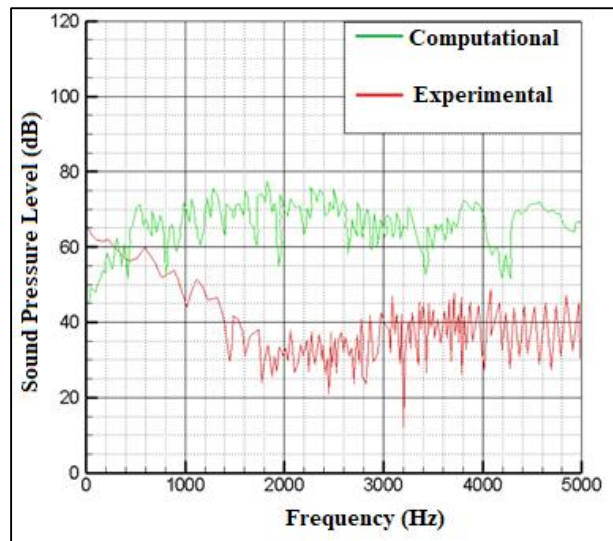

Figure 9: *Comparing the Results of the Analysis with the Experimental*

Sound Pressure Level obtained in our calculation was obtained at a higher level in decibels. We think that the reason for this difference is to use an insufficient number of a cell of mesh. In

our study, the network structure with around 2 million cells is used, but this is an insufficient number in wind turbine acoustic calculations. By determining the number of meshes around 10 million, the analysis should be carried out in this way. Figure 10 shows the comparison of the Sound Pressure Level obtained from the analysis where the wind velocity is 5.4 m/s and the results obtained from the analysis where the wind velocity is 7 m/s. When the results obtained from the analyses were examined, it was observed that the higher the wind entry speed, the higher the acoustic pressure produced.
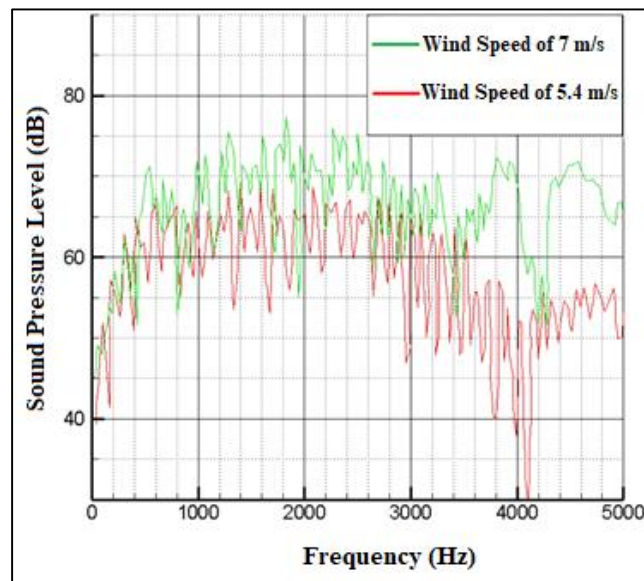

Figure 10: *Comparing the Results of the Analysis with Each Other*

5. Conclusions

In the research, URANS is examined to foretell aeroacoustic sound produced from the NREL Phase VI base scale. Furthermore, the effect of wind speeds on the acoustic result was investigated. The noise assessment is achieved by utilizing the pressure fluxes on the wind turbine blades calculated from URANS turbulence models set on computational fluid dynamics software. The wind turbine acoustics was calculated from the Lighthill equation, developed by Ffowcs-Williams and Hawkings. The aeroacoustic simulation outcomes were approved with test analysis. According to the obtained results, the analyzes made with URANS model cannot give very near results to the test data. Therefore, it is necessary to use turbulence models such as DES or LES, which can give more accurate results. Also, the results point out that the sound radiation from a wind turbine blade has a significant dependency on wind speed. It is demonstrated that a probability of decreasing the sound radiation with changing wind speed.

References

ANSYS FLUENT 12.0 Tutorial Guide

Avallone F., Velden W.C.P., Ragni D. (2017) Benefits of curved serrations on broadband trailing-edge noise reduction, Journal of Sound and Vibration, 400 : (2017), 167– 177. https://doi.org/10.1016/j.jsv.2017.04.007

Brooks T., Pope D., Marcolini M. (1989) Airfoil self-noise and prediction. Technical report, NASA Reference Publication 1218.

Cho T., Kim C., Lee D. (2009) Acoustic measurement for 12% scaled model of NREL Phase VI wind turbine by using beamforming, Current Applied Physics, 10:2010, 320-325. https://doi.org/10.1016/j.cap.2009.11.035

Ffowcs Williams J.E., Hawkings D.L. (1969). "Sound Generated by Turbulence and Surfaces in Arbitrary Motion," Philosophical Transactions of the Royal Society, Vol. 264, No. 11, 321-342. https://doi.org/10.1098/rsta.1969.0031

Global Wind Energy Council (2010), Global Wind Power Boom Continues Despite Economic Woes, [Online], Available from http://www.gwec.net [Accessed: 04 July 2019].

Jang-oh M., Young-ho L. (2011) Numerical simulation for prediction of aerodynamic noise characteristics on a HAWT of NREL phase VI, Mechanical Science and Technology. 1341- 1349. https://doi.org/10.1007/s12206-011-0234-1

Jianu O., Rosen M.A., Naterer G. (2012) Noise Pollution Prevention in Wind Turbines: Status and Recent Advances, Sustainability, 4(12):1104-1117. https://doi.org/10.3390/su4061104

Kepekci H., Zafer B., Guven H.R. (2018) Aeroacoustics Investigations of Unsteady 3D Airfoil for Different Angle Using Computational Fluid Dynamics Software, World Academy of Science, Engineering and Technology International Journal of Mechanical and Mechatronics Engineering, Vol:12, No:8.

Lighthill, M. J. (1952). On Sound generated aerodynamically General theory, Proceedings of the Royal Society, 211:1107. https://doi.org/10.1098/rspa.1952.0060

Morris P.J., Long L.N, Brentner K.S. (2004) An Aeroacoustic Analysis of Wind Turbines, 42nd AIAA Aerospace Sciences Meeting, and Exhibit, Reno, Nevada, 2004:1184, 1-11. https://doi.org/10.2514/6.2004-1184

Maizi M., Mohamed M.H., Dizene R., Mihoubi M.C. (2017) Noise reduction of a horizontal wind turbine using different blade shapes, Renewable Energy, 117: (2018), 242- 256. https://doi.org/10.1016/j.renene.2017.10.058

Maizi M., Dizene R., Mihoubi M.C. (2017) Reducing Noise Generated from a Wind Turbine Blade by Pitch Angle Control using CFD and Acoustic Analogy, Journal of Applied Fluid Mechanics, 10:4, 1201-1209. https://doi.org/10.18869/acadpub.jafm.73.241.27426

Menter F.R. (1994) Two-Equation Eddy-Viscosity Turbulence Models for Engineering Applications. AIAA Journal, 32:8, 1598- 1605. https://doi.org/10.2514/3.12149

Oerlemans S., Sijtsma P., and Lopez B. (2007) Location and quantification of noise sources on a wind turbine of sawtooth and slitted trailing edge geometries. Journal of Sound and Vibration, 299(4-5):869–883. https://doi.org/10.1016/j.jsv.2006.07.032

Rooks J. (2016) Computational aeroacoustic analysis of trailing edge noise, Master of Science Thesis, Delft University of Technology.

Sargolzaei J. (2007) Prediction of the power ratio and torque in wind turbine Savonius rotors using artificial neural networks, Proceedings of the WSEAS International Conference on Renewable Energy Sources, Arcachon, France, 7-13.

Schultz, K. (1994). Aeroacoustic Calculation of Helicopter Rotors at DLR.Proc, AGARD FDP Symposium on Aerodynamics and Aeroacoustics of Rotorcraft, CP552, Berlin-Germany, 10-13.

Tadamasa A., Zangeneh M. (2011) Numerical prediction of wind turbine noise, Renewable Energy, 1902-1912. https://doi.org/10.1016/j.renene.2010.11.036

Velden W.C.P., Pröbsting S., Zuijlen A.H., Jong A.T., Guan Y., Morris S.C. (2016). Numerical and experimental investigation of a beveled trailing-edge flow field and noise emission, Journal of Sound and Vibration, 384 (2016), 113–129. https://doi.org/10.1016/j.jsv.2016.08.005

Wasala S., Storey R., Norris S., Cater J. (2015) Aeroacoustic noise prediction for wind turbines using Large Eddy Simulation, Journal of Wind Engineering and Industrial Aerodynamics, 145:17-28. https://doi.org/10.1016/j.jweia.2015.05.011

Worasınchai S. (2012) Small Wind Turbine Starting Behaviour, Durham theses, Durham University.